

# TRANSPORT PROCESSES AND NEUTRINO EMISSION PROCESSES IN THE INTERIOR OF WHITE DWARFS

Naoki Itoh

Department of Physics, Sophia University  
7-1, Kioi-cho, Chiyoda-ku, Tokyo 102 Japan

ABSTRACT. Recent developments in the studies of the transport processes and the neutrino emission processes in the interior of white dwarfs are reviewed. Special emphasis is placed upon the accuracy of the calculations. Ionic correlation effects play an essential role in the transport processes and the neutrino bremsstrahlung process. The Weinberg-Salam theory is the basis for the calculation of the neutrino emission processes.

## 1. INTRODUCTION

Transport processes and neutrino emission processes are the key elements in the calculation of the evolution of white dwarfs. Recent developments in plasma physics and high energy physics have made accurate calculations of the transport processes and the neutrino emission processes possible. In this paper we review the recent developments in the studies of the transport processes and the neutrino emission processes in the interior of white dwarfs.

## 2. TRANSPORT PROCESSES

Recent papers on the transport processes in the interior of white dwarfs include Flowers and Itoh (1976,1979,1981), Yakovlev and Urpin (1980), Raikh and Yakovlev (1982), Itoh et al. (1983), Mitake, Ichimaru, and Itoh (1984), Itoh et al. (1984c), Nandkumar and Pethick (1984), Itoh, Kohyama, and Takeuchi (1987).

### 2.1 Electrical and thermal conductivities of dense matter in the liquid metal phase

Essential ingredients that go into accurate calculations of the transport properties of the dense matter include the inter-ionic correlations brought about by the strong Coulomb coupling and the electron-ion interaction represented by the screening function of the electrons. Our understanding of such many-particle effects in the

Coulomb system has progressed remarkably during the period of those developments due mainly to the advancement in the Monte Carlo method and other theoretical means (see, e.g., Ichimaru 1982). In this section we take account of what we consider to be the most reliable results currently available on the description of those many-particle effects, and thereby present an accurate calculation of the electrical and thermal conductivities of dense matter limited by electron-ion scattering in the liquid metal phase.

We shall consider the case that the atoms are completely pressure-ionized. We further restrict ourselves to the density-temperature region in which electrons are strongly degenerate. This condition is expressed as

$$T \ll T_F = 5.930 \times 10^9 \left[ \left( 1 + 1.1018(Z/A)^{2/3} \rho_6^{2/3} \right)^{1/2} - 1 \right] \text{ [K]}, \quad (1)$$

where  $T_F$  is the Fermi temperature,  $Z$  the atomic number of the nucleus, and  $\rho_6$  the mass density in units of  $10^6 \text{ g cm}^{-3}$ . For the ionic system we consider the case that it is in the liquid state. The latest criterion corresponding to this condition is given by (Slattery, Doolen, and Dewitt 1982)

$$\Gamma \equiv \frac{Z^2 e^2}{a k_B T} = 2.275 \times 10^{-1} \frac{Z^2}{T_8} \left( \frac{\rho_6}{A} \right)^{1/3} < 178, \quad (2)$$

where  $a = [3/(4\pi n_i)]^{1/3}$  is the ion-sphere radius, and  $T_8$  the temperature in units of  $10^8 \text{ K}$ .

In the present calculation we restrict ourselves to the cases where the high-temperature classical limit is applicable to the description of the ionic system. Specifically we assume that the parameter

$$y \equiv \frac{\hbar^2 k_F^2}{2M k_B T} = 1.656 \times 10^{-2} \frac{1}{A T_8} \left( \frac{Z}{A} \right)^{2/3} \rho_6^{2/3} \quad (3)$$

is much less than unity, where  $k_F$  is the Fermi wave number of the electrons and  $M$  is the mass of an ion. In Figure 1, we show the parameter domain for the validity of the present calculation in the case of  $^{56}\text{Fe}$  plasma.

For the calculation of the electrical and thermal conductivities we use the Ziman formula (1961) as is extended to the relativistically degenerate electrons (Flowers and Itoh 1976). On deriving the formula we retain the dielectric screening function due to the degenerate electrons. As to the explicit expression for the

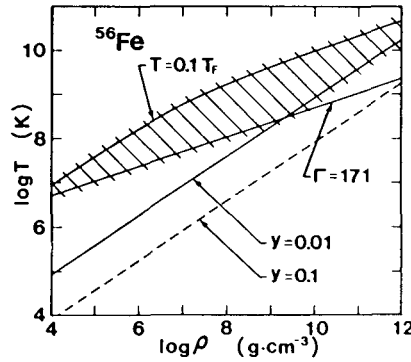


FIG.1. Parameter domain(shaded area) for the validity of the present calculation in the case of  $^{56}\text{Fe}$  plasma.

dielectric function, we use the relativistic formula worked out by Jancovici (1962). The use of the relativistic dielectric function is an essential difference between the present work and that of Yakovlev and Urpin (1980). Yakovlev and Urpin set the dielectric function due to electrons equal to unity; this assumption is valid only in the high-density limit.

Working on the transport theory for relativistic electrons given by Flowers and Itoh (1976), we obtain the expression for the electrical conductivity  $\sigma$  :

$$\sigma = 8.693 \times 10^{21} \frac{\rho_6}{A} \frac{1}{[1+1.018(Z/A)^{2/3} \rho_6^{2/3}] \langle S \rangle} \quad [\text{s}^{-1}]. \quad (4)$$

Here the scattering integral  $\langle S \rangle$  is evaluated for  $y \ll 1$  as

$$\begin{aligned} \langle S \rangle &= \int_0^1 d\left(\frac{k}{2k_F}\right) \left(\frac{k}{2k_F}\right)^3 \frac{S(k/2k_F)}{[(k/2k_F)^2 \epsilon(k/2k_F, 0)]^2} \\ &- \frac{1.018(Z/A)^{2/3} \rho_6^{2/3}}{1+1.018(Z/A)^{2/3} \rho_6^{2/3}} \int_0^1 d\left(\frac{k}{2k_F}\right) \left(\frac{k}{2k_F}\right)^5 \frac{S(k/2k_F)}{[(k/2k_F)^2 \epsilon(k/2k_F, 0)]^2} \\ &\equiv \langle S_{-1} \rangle - \frac{1.018(Z/A)^{2/3} \rho_6^{2/3}}{1+1.018(Z/A)^{2/3} \rho_6^{2/3}} \langle S_{+1} \rangle, \end{aligned} \quad (5)$$

where  $\hbar k$  is the momentum transferred from the ionic system to an electron,  $S(k/2k_F)$  the ionic structure factor, and  $\epsilon(k/2k_F, 0)$  the static dielectric screening function due to degenerate electrons. The first term in equation (5) corresponds to the ordinary Coulomb logarithmic term, and the second term is a relativistic correction term.

For the ionic liquid structure factor we use the results of the

improved hypernetted chain (IHNC) theory for the classical one-component plasma (Iyetomi and Ichimaru 1982).

For the thermal conductivity  $\kappa$  for relativistically degenerate electrons we analogously obtain the expression:

$$\kappa = 2.363 \times 10^{17} \frac{\rho_6 T_8}{A} \frac{1}{[1 + 1.018(Z/A)^{2/3} \rho_6^{2/3}] \langle S \rangle} \quad [\text{ergs cm}^{-1} \text{ s}^{-1} \text{ K}^{-1}] \quad (6)$$

where  $\langle S \rangle$  is the same as that for electrical conductivity.

We have carried out the integrations in equation (5) numerically by using the IHNC structure factor of the classical one-component plasma and Jancovici's (1962) relativistic dielectric function for degenerate electrons. We have made calculations for the parameter ranges  $2 \leq \Gamma \leq 160$ ,  $10^{-4} \leq r_s \leq 0.5$ , which cover most of the density-temperature region of the dense matter in the liquid metal phase of astrophysical importance.

In Figures 2,3,4, and 5 we compare the results of the calculation of  $\langle S \rangle$  by Yakovlev and Urpin (1980) (dashed curves) with the present results (solid curves). For the  $^1\text{H}$  matter and the  $^4\text{He}$

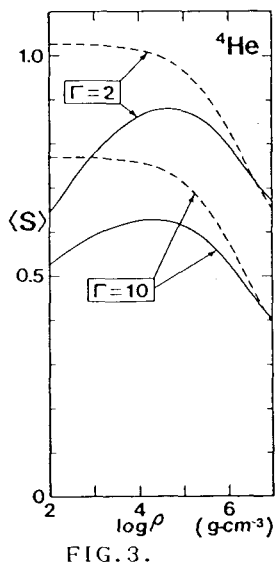
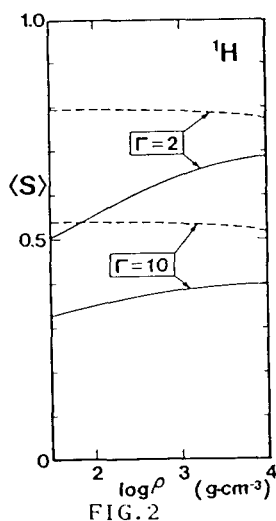


FIG.2. Comparison of Yakovlev and Urpin's results(dashed curves) with the present results(solid curves) for the  $^1\text{H}$  matter.

FIG.3. Same as FIG.2. for the  $^4\text{He}$  matter.

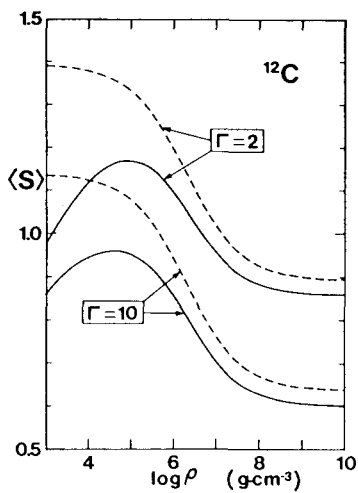


FIG. 4.

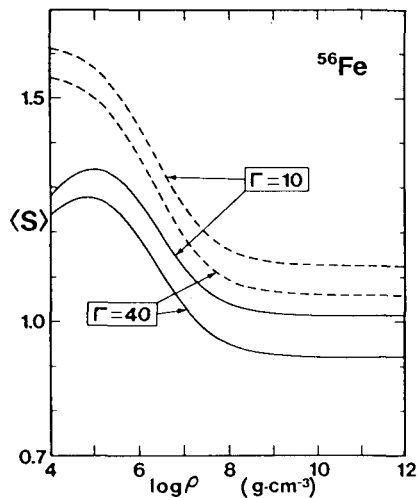


FIG. 5.

FIG. 4. Same as FIG. 2. for the  $^{12}\text{C}$  matter.

FIG. 5. Same as FIG. 2. for the  $^{56}\text{Fe}$  matter.

matter Yakovlev and Urpin's results amount to an overestimation of  $\langle S \rangle$  by 60% at low densities. For the  $^{12}\text{C}$  matter their overestimation of  $\langle S \rangle$  amounts to 40% at low densities. For the  $^{56}\text{Fe}$  matter their overestimation is nearly 30% at low densities. At high densities Yakovlev and Urpin's results are reasonably close to the present ones. The large amount of the overestimation of  $\langle S \rangle$  at low densities by Yakovlev and Urpin is due to their neglect of electron screening. At high densities, however, the effect of the screening due to electrons is relatively small. This is the main reason for their overestimation of the resistivity (underestimation of the conductivity) at low densities.

## 2.2 Electrical and thermal conductivities of dense matter in the crystalline lattice phase

In this section we deal with the electrical and thermal conductivities of dense matter in the crystalline lattice phase  $\Gamma > 178$ . The electrical conductivity  $\sigma$  and thermal conductivity  $\kappa$  are related to the effective electron collision frequencies  $\nu_\sigma$  and  $\nu_\kappa$  by

$$\sigma = \frac{e^2 n_e}{m^* \nu_\sigma} = 1.525 \times 10^{20} \frac{Z}{\text{A}} \rho_6 \left[ 1 + 1.018 \left( \frac{Z}{\text{A}} \rho_6 \right)^{2/3} \right]^{-1/2} \times \frac{10^{18} \text{ s}^{-1}}{\nu_\sigma} \text{ s}^{-1}, \quad (7)$$

$$\kappa = \frac{\pi^2 k_B^2 T n_e}{3 m^* \nu_\kappa} = 4.146 \times 10^{15} \frac{Z}{A} \rho_6 [1 + 1.018 \left(\frac{Z}{A} \rho_6\right)^{2/3}]^{-1/2} \\ \times T_8 \frac{10^{18} \text{ s}^{-1}}{\nu_\kappa} \text{ ergs cm}^{-1} \text{ s}^{-1} \text{ K}^{-1}, \quad (8)$$

where  $n_e$  is the number density of electrons and  $m^*$  is the relativistic effective mass of an electron at the Fermi surface. In this section we are interested in the scattering of electrons by phonons. The collision frequencies  $\nu_\sigma$  and  $\nu_\kappa$  due to one-phonon processes can be calculated by the variational method (Flowers and Itoh 1976; Yakovlev and Urpin 1980; Raikh and Yakovlev 1982) as

$$\nu_{\sigma, \kappa} = \frac{e^2}{\hbar \nu_F} \frac{k_B T_{F, \sigma, \kappa}}{\hbar} = 9.554 \times 10^{16} T_8 \left\{ 1 + \frac{1}{1.018 [(Z/A) \rho_6]^{2/3}} \right\}^{1/2} \\ \times F_{\sigma, \kappa} \text{ s}^{-1}, \quad (9)$$

$$F_{\sigma, \kappa} = \frac{2\gamma^2}{S^2} \int \frac{dS dS'}{k^4 |\epsilon(k, 0)|^2} \left[ 1 - \left(\frac{\beta k}{2k_F}\right)^2 \right] e^{-2W(k)} |f(k)|^2 \\ \times \sum_{s=1}^3 [k \cdot \hat{\epsilon}_s(p)]^2 (e^{Zs} - 1) - 2e^{Zs} g_{\sigma, \kappa} \quad (10)$$

In the above the integral is over the areas of the Fermi surface,  $k$  is the momentum transfer,  $\hat{\epsilon}_s(p)$  the polarization unit vector of a phonon with momentum  $p$  and polarization  $s$ , and

$$\gamma \equiv \frac{\hbar \omega_p}{k_B T} = 7.832 \times 10^{-2} \frac{Z}{(AA')^{1/2}} \frac{\rho_6^{1/2}}{T_8} = 0.3443 \frac{\rho_6^{1/6}}{A^{1/6} (A')^{1/2} Z} \Gamma, \quad (11)$$

$$\beta \equiv \frac{\hbar k_F c}{E_F} = \left\{ 1 + \frac{1}{1.018 [(Z/A) \rho_6]^{2/3}} \right\}^{-1/2}, \quad (12)$$

$$Z_s \equiv \frac{\hbar \omega_s(p)}{k_B T}, \quad (13)$$

$$g_\sigma = k^2, \quad (14)$$

$$g_\kappa = k^2 - \frac{k^2 Z_s^2}{2\pi^2} + \frac{3k_F Z_s^2}{\pi^2}, \quad (15)$$

$\omega_p$  being the ionic plasma frequency. The momentum conservation requires  $k = \pm p + K$ , where  $K$  is the reciprocal-lattice vector for the Brillouin zone to which  $k$  is confined. In equation (10) we have included the dielectric screening function due to relativistically

degenerate electrons  $\varepsilon(k,0)$ , the Debye-Waller factor  $e^{-2W(k)}$ , and the atomic form factor  $f(k)$ . Yakovlev and Urpin (1980) and Raikh and Yakovlev (1982) have used the Thomas-Fermi screening and set  $e^{-2W(k)}=1$ ,  $f(k)=1$ .

The phonon spectra are modified by the screening due to electrons. The longitudinal optical phonon turns into an acoustic phonon in the long-wavelength limit, whereas the original transverse acoustic phonons are little affected by the electron screening (Pollock and Hansen 1973). Because the low-frequency transverse phonons play dominant roles in the resistivity of dense stellar matter, we neglect the effects of the electron screening on the phonon spectra and use the frequency moment sum rules for the pure Coulomb lattice.

As we consider the case in which the Fermi sphere is much larger than the Debye sphere,  $(k_F/k_D)^3=Z/2 \gg 1$ , Umklapp processes contribute to the scattering dominantly, and the vector  $k$  in equation (10) most probably falls in a Brillouin zone distant from the first zone. When we perform an integration within a single distant zone corresponding to the reciprocal-lattice vector  $K$ , we can make an approximation  $k=K$  in the integrand and carry out an integration over  $p$  within the first zone only.

Here we follow the semianalytical approach adopted by Yakovlev and Urpin (1980) and also by Raikh and Yakovlev (1982). We write

$$\sum_{S=1}^3 [k \cdot \hat{\varepsilon}_S(p)]^2 Z_S^n (e^{Z_S} - 1)^{-2} e^{Z_S} \approx \frac{\pi n k^2}{\gamma^2} G^{(n)}(\gamma), \quad (16)$$

$$G^{(n)}(\gamma) = \frac{\gamma^2}{3V_B \pi n} \sum_{S=1}^3 \int dp Z_S^n (e^{Z_S} - 1)^{-2} e^{Z_S}, \quad (17)$$

where  $n=0$  or  $2$ , and integration is carried out over the first Brillouin zone, whose volume is  $V_B$ . By the use of this approximation  $F_\sigma$  and  $F_\kappa$  in equation (10) are expressed as

$$F_\sigma = I_\sigma G^{(0)}(\gamma), \quad (18)$$

$$F_\kappa = I_\sigma G^{(0)}(\gamma) + I_\kappa^{(2)} G^{(2)}(\gamma), \quad (19)$$

$$I_\sigma = \int_{-1}^{\mu} \max d\mu \frac{e^{-2W(q)} |f(q)|^2}{|\varepsilon(q,0)|^2} (1 - \beta^2 q^2), \quad (20)$$

$$I_{\kappa}^{(2)} = \int_{-1}^{\mu_{\max}} d\mu \frac{e^{-2W(q)} |f(q)|^2}{q^2 |\varepsilon(q,0)|^2} (1 - \beta^2 q^2) \left( -\frac{1}{2} q^2 + \frac{3}{4} \right), \quad (21)$$

$$q = \left( \frac{1-\mu}{2} \right)^{1/2}, \quad (22)$$

$$q_{\min} = \left( \frac{1-\mu_{\max}}{2} \right)^{1/2}, \quad (23)$$

$$\mu_{\max} = 1 - 0.3575Z^{-2/3}. \quad (24)$$

Here we have introduced a small momentum transfer cutoff  $q_{\min}$  corresponding to the unavailability of Umklapp processes for  $q < q_{\min}$ . The contributions of the normal processes are very much smaller than those of the Umklapp processes. For the choice of  $q_{\min}$  we follow Raikh and Yakovlev (1982). Yakovlev and Urpin (1980) derived the asymptotic expressions of  $G^{(0)}(\gamma)$  and  $G^{(2)}(\gamma)$  for  $\gamma \ll 1$  and  $\gamma \gg 1$ , and proposed the following analytic formulae for arbitrary  $\gamma$ , which fit the main terms of the asymptotic expressions:

$$G^{(0)}(\gamma) = u_{-2} \left[ 1 + \left( \frac{3u_{-2}\gamma^2}{\pi^2 c_2} \right)^2 \right]^{-1/2} \approx 13.00 (1 + 0.0174\gamma^2)^{-1/2}, \quad (25)$$

$$G^{(2)}(\gamma) = \frac{\gamma^2}{\pi^2} \left[ 1 + \left( \frac{15}{4\pi^4 c_2} \right)^{2/3} \right]^{-3/2} = \frac{\gamma^2}{\pi^2} (1 + 0.0118\gamma^2)^{-3/2}, \quad (26)$$

where  $u_{-2} \approx 13.00$  (Pollock and Hansen 1973) and  $c_2 = 29.98$  (Coldwell-Horsfall and Maradudin 1960) are the numerical constants that are characteristic of the phonon spectrum of the bcc Coulomb lattice. Raikh and Yakovlev (1982) calculated  $G^{(0)}(\gamma)$  and  $G^{(2)}(\gamma)$  numerically with the exact spectrum of phonons for  $\gamma < 100$ . It has been confirmed that the fitting formulae (25) and (26) have an accuracy better than 10% even at  $\gamma \sim 1$ .

We have carried out the numerical integrations of equations (20) and (21) for  ${}^4\text{He}$ ,  ${}^{12}\text{C}$ ,  ${}^{16}\text{O}$ ,  ${}^{20}\text{Ne}$ ,  ${}^{24}\text{Mg}$ ,  ${}^{28}\text{Si}$ ,  ${}^{32}\text{S}$ ,  ${}^{40}\text{Ca}$ ,  ${}^{56}\text{Fe}$ . Some of the results are presented in Figures 6-9. For comparison we have also included the case where we have neglected the effects of the Debye-Waller factor and set  $e^{-2W} = 1$ . We also show the results of Raikh and Yakovlev (1982) which are

$$[I_{\sigma}]_{\text{RY}} = 2 - \beta^2, \quad (27)$$

$$[I_{\kappa}^{(2)}]_{\text{RY}} = \ln Z - \beta^2 + 1.583. \quad (28)$$

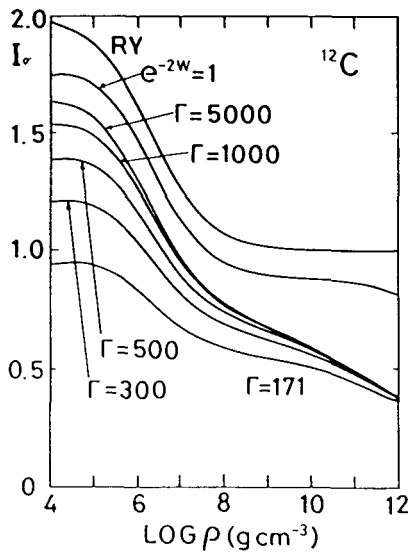


FIG. 6.

FIG. 6.  $I_{\sigma}$  for the  $^{12}\text{C}$  matter. RY stands for the results of Raikh and Yakovlev(1982).

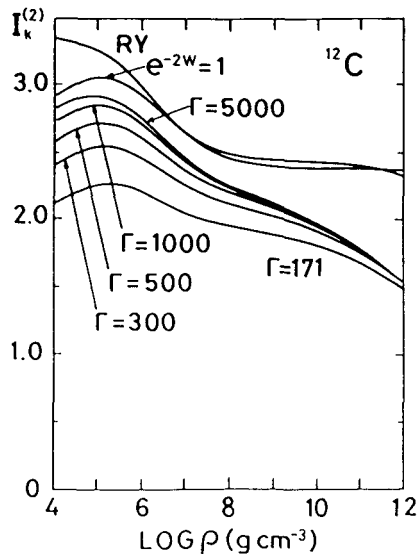


FIG. 7.

FIG. 7.  $I_{\kappa}^{(2)}$  for the  $^{12}\text{C}$  matter.

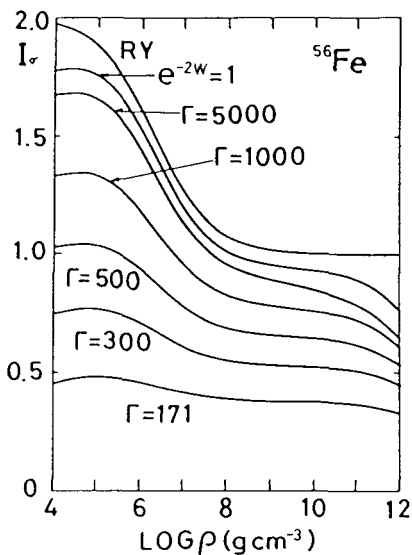


FIG. 8.

FIG. 8.  $I_{\sigma}$  for the  $^{56}\text{Fe}$  matter.

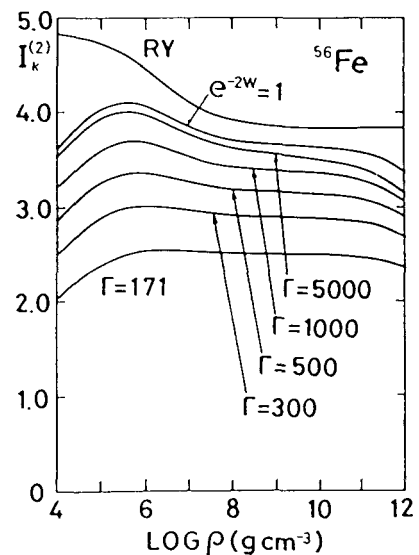


FIG. 9.

FIG. 9.  $I_{\kappa}^{(2)}$  for the  $^{56}\text{Fe}$  matter.

It is readily seen that the Debye-Waller factor reduces the resistivities (enhances the conductivities) by a factor of 2-4 near the melting temperature. This means that the results of Yakovlev and Urpin (1980) and those of Raikh and Yacovlev (1982) give too low conductivities by that factor. It is very interesting to observe that the present result is fortuitously rather close to the original Flowers-Itoh conductivity in the crystalline lattice phase near the melting temperature (Flowers and Itoh 1976,1981).

### 3. NEUTRINO EMISSION PROCESSES

Recent papers on the neutrino energy loss rates include Munakata, Kohyama, and Itoh (1985), Kohyama, Itoh, and Munakata (1986), Itoh, and Kohyama (1983), Itoh et al. (1984d), Itoh et al. (1984a), Itoh et al. (1984b), Munakata, Kohyama, and Itoh (1987), Schinder et al. (1987), and Itoh et al. (1988).

#### 3.1 Photoneutrino process

The energy loss rate per unit volume per unit time due to the photoneutrino process is expressed as (Munakata, Kohyama, and Itoh 1985)

$$Q_{\text{photo}} = \frac{1}{2} [(C_V^2 + C_A^2) + n(C_V'^2 + C_A'^2)] Q_{\text{photo}}^+ - \frac{1}{2} [(C_V^2 - C_A^2) + n(C_V'^2 - C_A'^2)] Q_{\text{photo}}^- , \quad (29)$$

$$C_V = 1/2 + 2\sin^2\theta_w , \quad C_A = 1/2 , \quad (30)$$

$$C_V' = 1 - C_V , \quad C_A' = 1 - C_A , \quad (31)$$

$$\sin^2\theta_w = 0.23 , \quad (32)$$

where  $\theta_w$  is the Weinberg angle, and  $n$  is the number of the neutrino flavors other than the electron neutrino whose masses can be neglected compared with  $k_B T$ .

As in Munakata, Kohyama, and Itoh (1985) we have carried out Monte Carlo computations, using the method of importance sampling, to evaluate the five-dimensional integral which appears in  $Q_{\text{photo}}^+$  and  $Q_{\text{photo}}^-$ . In all the calculations of the photoneutrino process we used 50000 random points. Schinder et al. (1987) used 50000 random points for the calculations corresponding to the temperatures  $T=10^8, 10^9, 10^{10}, 10^{11}$  K, and they used 5000 random points for the other temperatures.

### 3.2 Pair neutrino process

The energy loss rate due to the pair neutrino process is expressed as (Munakata, Kohyama, and Itoh 1985)

$$Q_{\text{pair}} = \frac{1}{2} [(C_V^2 + C_A^2) + n(C_V'^2 + C_A'^2)] Q_{\text{pair}}^+ + \frac{1}{2} [(C_V^2 - C_A^2) + n(C_V'^2 - C_A'^2)] Q_{\text{pair}}^- \quad (33)$$

At high temperatures ( $T > 10^9$  K), the energy loss rate due to the pair neutrino process is independent of the density and dominates over the other processes.

### 3.3 Plasma neutrino process

Kohyama, Itoh, and Munakata (1986) have shown that the axial-vector contribution to the plasma neutrino energy loss rate is at most on the order of 0.01% of the vector contribution for  $T \leq 10^{11}$  K. Thus for practical purposes the axial-vector contribution can be safely neglected. Therefore the energy loss rate due to the plasma neutrino process is written as

$$Q_{\text{plasma}} = (C_V^2 + n C_V'^2) Q_V \quad (34)$$

The expression for  $Q_V$  has been given by Beaudet, Petrosian, and Salpeter (1967) and also by Kohyama, Itoh, and Munakata (1986).

### 3.3 Bremsstrahlung neutrino process

The calculation of the neutrino energy loss rate due to the bremsstrahlung neutrino process has been carried out in the two different regions: the region in which electrons are strongly degenerate and the region in which electrons are partially degenerate.

In the first region we can take into account the ionic correlation accurately. The calculation of the bremsstrahlung neutrino energy loss rate based on the Weinberg-Salam theory which takes into account the ionic correlation fully has been reported by Itoh and Kohyama (1983), Itoh et al. (1984d), Itoh et al. (1984a), and Itoh et al. (1984b).

For the density-temperature region in which electrons are partially degenerate, Munakata, Kohyama, and Itoh (1987) have calculated the energy loss rate in the framework of the Weinberg-Salam theory.

### 3.4 Comparison of various neutrino processes

In Figures 10-14 we show the contributions of the various neutrino processes for the case of  $\sin^2\theta_w=0.23$ ,  $n=2$ , and  $^{56}\text{Fe}$  matter corresponding to the temperatures  $T=10^7, 10^8, 10^9, 10^{10}, 10^{11}$  K. In Figure 15 we show the most dominant neutrino process for a given density and temperature for the case of  $n=2$  and  $^{56}\text{Fe}$  matter. In Figure 16 we show the contours of the constant total neutrino energy loss

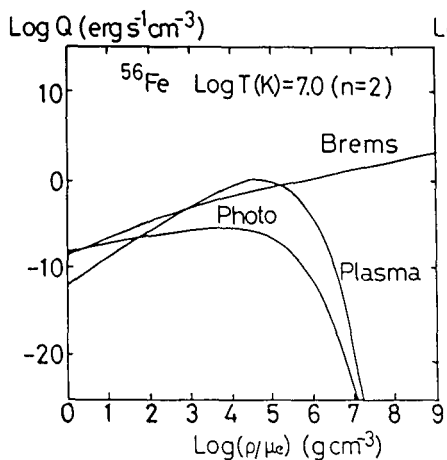


FIG.10.

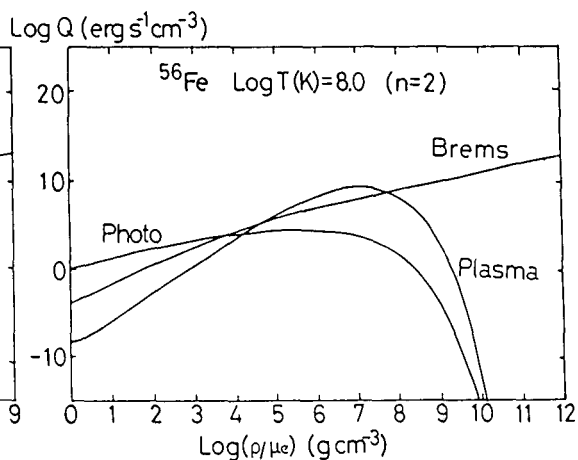


FIG.11.

FIG.10. Neutrino energy loss rates due to photo-, plasma, and bremsstrahlung processes for  $n=2$ ,  $^{56}\text{Fe}$  matter,  $T=10^7$  K.

FIG.11. Same as FIG.10. but including pair neutrino process, for  $T=10^8$  K.

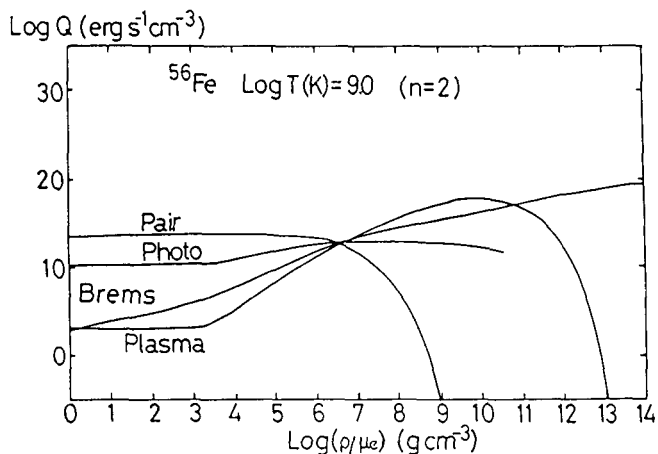


FIG.12. Same as FIG.11. for  $T=10^9$  K.

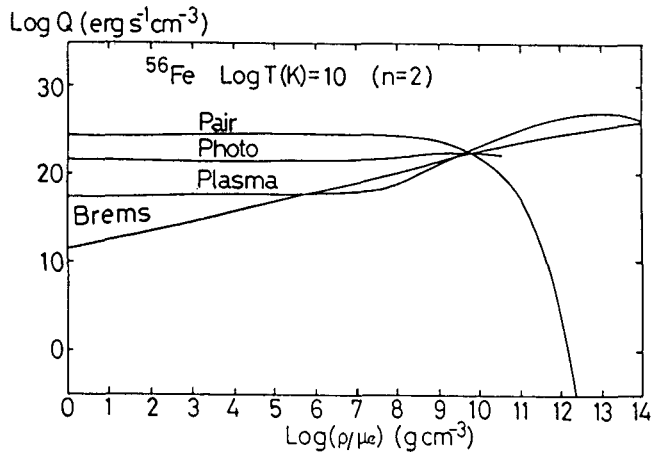


FIG.13. Same as FIG.11. for  $T=10^{10}$  K.

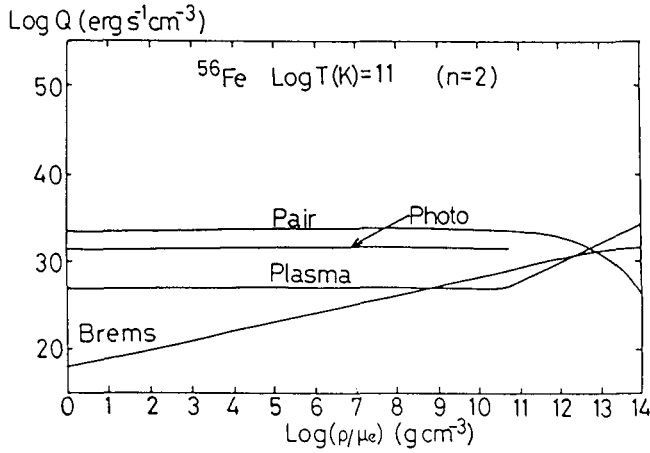


FIG.14. Same as FIG.11. for  $T=10^{11}$  K.

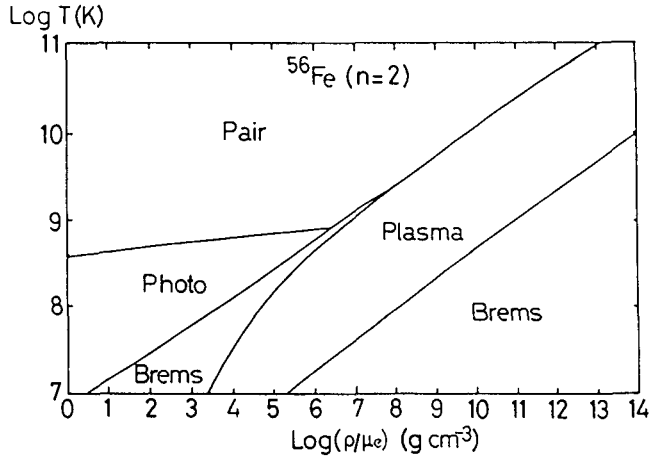


FIG.15. Most dominant neutrino process for a given density and temperature for the case of  $n=2$  and  $^{56}\text{Fe}$  matter.

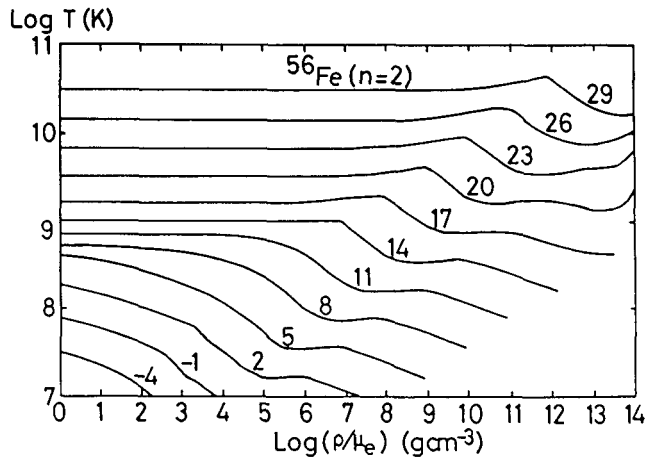


FIG.16. Contours of the constant total neutrino energy loss rates due to pair, photo-, plasma, and bremsstrahlung processes for the case of  $n=2$  and  $^{56}\text{Fe}$  matter,  $\log Q \text{ (erg s}^{-1} \text{ cm}^{-3}\text{)} = \text{const.}$

rates due to pair, photo-, plasma, and bremsstrahlung processes for the case of  $n=2$  and  $^{56}\text{Fe}$  matter.

#### 4. CONCLUDING REMARKS

The transport processes and the neutrino emission processes in the interior of white dwarfs determine the structure and evolution of white dwarfs. The recent developments in this field reviewed in this article are expected to elucidate the comparison of the observations of white dwarfs with the theoretical studies. It is interesting to quote the following:

“Observe me well, Princess, before you give me your word,” said the Yellow Dwarf.

The classic fairy tales

I would make a parody of this as follows:

“Observe me well, Astronomers, before you give me your word,” said the White Dwarf.

The modern fairy tales

#### REFERENCES

- Beudet, G., Petrosian, V., and Salpeter, E.E. 1967, *Ap.J.*, 150, 979.  
 Coldwell-Horsfall, R.A., and Maradudin, A.A. 1960, *J.Math.Phys.*, 1, 395.  
 Flowers, E., and Itoh, N. 1976, *Ap.J.*, 206, 218.

- Flowers, E., and Itoh, N. 1979, *Ap.J.*, 230, 847.
- Flowers, E., and Itoh, N. 1981, *Ap.J.*, 250, 750.
- Ichimaru, S. 1982, *Rev.Mod.Phys.*, 54, 1017.
- Itoh, N., Adachi, T., Nakagawa, M., Kohyama, Y., and Munakata, H. 1988, submitted to *Ap.J.*
- Itoh, N., and Kohyama, Y. 1983, *Ap.J.*, 275, 858.
- Itoh, N., Kohyama, Y., Matsumoto, N., and Seki, M. 1984a, *Ap.J.*, 280, 787.
- Itoh, N., Kohyama, Y., Matsumoto, N., and Seki, M. 1984b, *Ap.J.*, 285, 304; 322, 584 (1987).
- Itoh, N., Kohyama, Y., Matsumoto, N., and Seki, M. 1984c, *Ap.J.*, 285, 758.
- Itoh, N., Kohyama, Y., and Takeuchi, H. 1987, *Ap.J.*, 317, 733.
- Itoh, N., Matsumoto, N., Seki, M., and Kohyama, Y. 1984d, *Ap.J.*, 279, 413.
- Itoh, N., Mitake, S., Iyetomi, H., and Ichimaru, S. 1983, *Ap.J.*, 273, 774.
- Iyetomi, H., and Ichimaru, S. 1982, *Phys.Rev.*, A25, 2434.
- Jancovici, B. 1962, *Nuovo Cimento*, 25, 428.
- Kohyama, Y., Itoh, N., and Munakata, H. 1986, *Ap.J.*, 310, 815.
- Mitake, S., Ichimaru, S., and Itoh, N. 1984, *Ap.J.*, 277, 375.
- Munakata, H., Kohyama, Y., and Itoh, N. 1985, *Ap.J.*, 296, 197; 304, 580 (1986).
- Munakata, H., Kohyama, Y., and Itoh, N. 1987, *Ap.J.*, 316, 708.
- Nandkumar, R., and Pethick, C.J. 1984, *M.N.R.A.S.*, 209, 511.
- Pollock, E.L., and Hansen, J.P. 1973, *Phys.Rev.*, A8, 3110.
- Raiikh, M.E., and Yakovlev, D.G. 1982, *Ap.Space Sci.*, 87, 193.
- Schinder, P.J., Schramm, D.N., Wiita, P.J., Margolis, S.H., and Tubbs, D.L. 1987, *Ap.J.*, 313, 531.
- Slattery, W.L., Doolen, G.D., and Dewitt, H.E. 1982, *Phys.Rev.*, A26, 2255.
- Yakovlev, D.G., and Urpin, V.A. 1980, *Soviet Astr.*, 24, 303.
- Ziman, J. 1961, *Phil.Mag.*, 6, 1013.